Rotationally Resolved Electronic Spectra of 1,2-Dimethoxybenzene and the 1,2-Dimethoxybenzene−Water Complex

John T. Yi, Jason W. Ribblett,† and David W. Pratt*

Department of Chemistry, University of Pittsburgh, Pittsburgh, Pennsylvania 15260

Received: June 16, 2005; In Final Form: August 12, 2005

Rotationally resolved $S_1 \leftarrow S_0$ electronic spectra of 1,2-dimethoxybenzene (DMB) and its water complex have been observed and assigned. The derived values of the rotational constants show that the bare molecule has a planar heavy-atom structure with *trans*-disposed methoxy groups in its ground and excited electronic states. The 0_0^0 transition of DMB is polarized along the *b*-axis bisecting the methoxy groups, demonstrating that its S_1 state is an ^1L_b state. Higher energy bands of DMB are also polarized along the *b*-axis and have been tentatively assigned to different vibrational modes of the ^1L_b state. The water complex origin appears 127 cm^{-1} to the blue of the bare molecule origin. Analyses of the high resolution spectra of DMB/H_2O and DMB/D_2O suggest that the water molecule is attached *via* two O−H···O hydrogen bonds to the methoxy groups in both electronic states. A tunneling motion of the attached water molecule is revealed by a splitting of these spectra into two subbands. Potential barriers to this motion have been determined.

I. Introduction

Investigations of molecular conformers and their complexes continue to provide vital information about *intra*- and *inter*molecular forces. In this report, we focus on 1,2-dimethoxybenzene (DMB) and its hydrogen bonded complex with a single water molecule.

The conformational preferences of dimethoxy-substituted benzenes have been the subject of several studies.[1−7] Hill *et al.*[2] used near ultraviolet spectroscopy to determine the polarization directions of the ^1L_b and ^1L_a transitions of a series of homo- and heterodisubstituted benzene derivatives. In DMB, they found the polarization direction of the ^1L_b transition at 278 nm to be along the *z*-symmetry axis and the polarization direction of the ^1L_a transition at 227 nm to be along the *y*-axis, as shown in Scheme 1. Based on time-of-flight mass spectroscopy (TOFMS) experiments combined with dispersed emission results, Bernstein and co-workers proposed that DMB in the gas phase is probably planar in nature.[5] The lower excited state frequency bands were also analyzed utilizing isotopic substitution; these were assigned to torsional motions of the methoxy groups.

SCHEME 1: Symmetry Axes of DMB

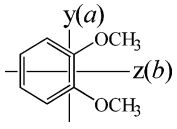

There have been no previous reports of a DMB/water complex. However, other hydrogen bonded aromatic molecule/water complexes, particularly benzene and substituted benzene/water complexes, have been extensively studied. Currently,[8−10] it is believed that in benzene/water, the water forms hydrogen bonds with the π-electrons in an "a-top" binding site. In contrast, substituted benzene/water complexes display equilibrium structures in which the water lies in the plane of the aromatic ring.[11−18] Benzonitrile,[11,12] anisole,[13] and mono- and difluorobenzene[14−16] water complexes exhibit double hydrogen bonds. One hydrogen atom of the water molecule (the hydrogen donor) is bound to the substituent atom (H···X), whereas the oxygen atom of the water (the hydrogen acceptor) is bound to a hydrogen atom (H···OH_2) of the bare molecule. In phenol[17] and indole[18] clusters, the water (hydrogen acceptor) is bound to the electrophilic hydrogen atom of the bare molecule (H···OH_2). A molecular plane bisects the plane of the singly bonded water so that its hydrogens are out-of-plane.

In all such complexes, the attached water also undergoes a large amplitude motion with respect to the parent molecule. In benzene/water, Gutowsky *et al.*[8] showed that the plane of the water is 34° off the C_2 axis and rotates about the C_6 axis of benzene. Also, using resonant ion-dip infrared spectroscopy with resonant two-photon (R2PI) spectroscopy, Pribble *et al.*[9] recorded the infrared spectra of the O−H stretch of benzene−H_2O and showed that a large tumbling motion of water about the 6-fold axis of benzene occurs. Previous substituted benzene/water cluster studies have reported the observation of a variety of different types of motion of the attached water molecules. Studies of small molecule−H_2O complexes, such as H_2O-H_2O and CO−H_2O, also have revealed a variety of tunneling motions.[19,20]

In this work, we report the results of fluorescence excitation studies that shed light on the geometry and dynamical properties of DMB and its water complex in their S_0 and S_1 electronic states. First, the preferred structure of DMB will be determined in its ground and excited electronic states from fits of its rotationally resolved fluorescence excitation spectrum. This spectrum also gives information about the distribution of electrons in the ground state, and how this changes when the photon is absorbed. Second, tentative assignments of several low frequency bands that appear in this spectrum will be made based on their rotational constants and vibrational frequency calculations. Third, the preferred structure of the water complex of DMB will be determined from analysis of the corresponding

* Address correspondence to this author. E-mail: pratt@pitt.edu.
† Present address: Department of Chemistry, Ball State University, Muncie, IN 47306.

10.1021/jp053254l CCC: $30.25
Published on Web 10/05/2005

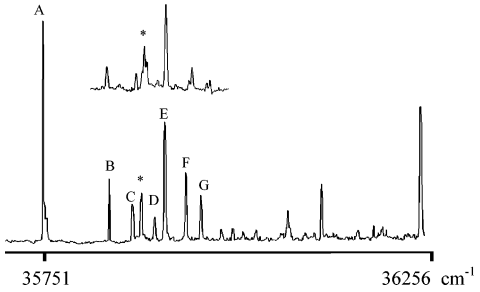

Figure 1. Vibrationally resolved fluorescence excitation spectrum of 1,2-dimethoxybenzene. The asterisk denotes a band that appears when H_2O is added to the sample; the insert shows how the spectrum of this band is changed when D_2O is added to the sample.

excitation spectra of DMB−H_2O and DMB-D_2O. The results show a new type of water (hydrogen donor) interaction involving the lone pair electrons of the oxygen atoms in DMB. Finally, information about the internal rotation dynamics of the attached water molecule will be obtained from an analysis of the perturbations that appear in these spectra.

II. Experimental Section

1,2-Dimethoxybenzene (veratrole) was purchased from Aldrich and purified by fractional distillation with CaH_2 under vacuum conditions. In the vibrationally resolved electronic experiment, the sample was seeded into 40 psi of He gas (premixed with H_2O or D_2O for the complex) and expanded into a vacuum chamber (10^{-5} Torr) through a 1 mm diameter pulsed nozzle (General Valve Series 9), operating at 10 Hz. One centimeter downstream of the valve, the sample was excited with the second harmonic of a Quanta Ray Nd^{3+}:YAG (Model DCR-1A) pumped dye laser (Model PDL-1). The dye (Fluorescein 548) laser output was frequency doubled with an external β-barium borate (BBO) crystal providing a spectral resolution of 0.6 cm^{-1} in the ultraviolet. From the point of intersection between the nozzle and laser, the molecules were excited and the fluorescence was collected with a photomultiplier tube. Finally, the collected data were processed by a boxcar integrator (Stanford Research Systems) and recorded with a DataAcq data acquisition system.

Rotationally resolved electronic experiments on DMB were performed using a CW laser spectrometer, described elsewhere.[21] Briefly, the sample was seeded into He gas (premixed with H_2O or D_2O for the complex), expanded through a 240 mm quartz nozzle, and probed 15 cm downstream of the nozzle by an Ar^+ pumped CW tunable dye laser. The CW laser operated with Rhodamine 110 dye; 100−200 μW of UV radiation was obtained by intracavity frequency doubling using a BBO 560 crystal. The fluorescence excitation spectrum, the iodine absorption spectrum, the relative frequency markers, and the laser output power were simultaneously collected and processed by a jb95a data acquisition system.[21] Transition frequencies were calibrated by comparison with the I_2 absorption spectrum and frequency markers from a stabilized etalon with a free spectral range of 299.7520 ± 0.0005 MHz.

TABLE 1: Absolute and Relative Energies of Several Low Frequency Bands that Appear in the $S_1 \leftarrow S_0$ Fluorescence Excitation Spectrum of DMB

Bands	Energy (cm^{-1})	Rel Energy (cm^{-1})	ΔI (amu Å)	Assignments[a]
A	35751	0	−7.68	
B	35835	84	−10.23	$2a_2^{\dagger}$ or $2b_1^{\dagger}$
C	35868	117	−9.46	$a_2^{\dagger}\,a_2^{\ddagger}$
D	35893	142	−9.06	$2b_1^{\ddagger}$
E	35902	151	−8.95	$2a_2^{\ddagger}$
F	35931	180	−8.87	$a_2^{\dagger}a_2^{\ddagger}$
G	35952	201	−7.50	a_1

[a] See Scheme 8 for a description of the individual vibrational modes.

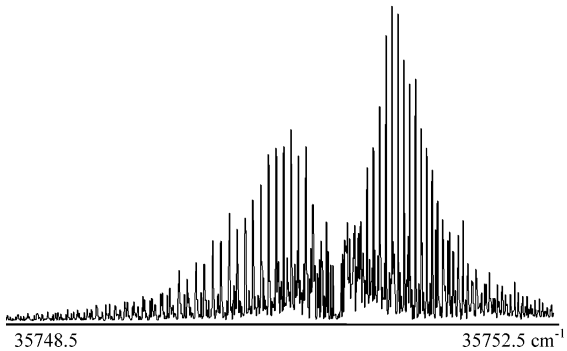

Figure 2. Rotationally resolved fluorescence excitation spectrum of Band A of DMB.

III. Results and Interpretation

The low resolution $S_1 \leftarrow S_0$ fluorescence excitation spectrum of DMB in a supersonic jet is shown in Figure 1. It exhibits several bands. Band A, at 35751 cm^{-1} (∼280 nm), has been identified as the electronic origin, or 0_0^0 band, of DMB.[6,22] This band is red shifted from the benzene origin due to conjugation of the benzene π-orbitals and methoxy nonbonding orbitals; the corresponding band of benzene is at 38091 cm^{-1} (∼260 nm).[23] Bands B−G, at relatively small displacements from the DMB origin, are unique to DMB. The bands at still higher displacements have analogues in benzene. For example, the band at 36254 cm^{-1} (0_0^0 + 503 cm^{-1}) in Figure 1 is the analogue of the 6_0^1 band in benzene.[23]

The bands of primary interest to us in Figure 1 are the origin band, Band A, and Bands B−G, which have no analogues in the spectrum of benzene. Table 1 lists the frequencies of these bands. Apparently, Bands B, C, and D form a progression beginning at 0_0^0 +84 cm^{-1}, and Bands E, F, and G form a similar progression beginning at 0_0^0 +151 cm^{-1}. If these are progressions, their nature (*i.e.*, the vibrational motions that are responsible for them) is unknown. It is also possible that these bands are the bands of different conformers of DMB whose origins are shifted in frequency by different amounts.

Also of interest is the band marked with an asterisk in Figure 1, at 0_0^0 +127 cm^{-1}. This band grows in intensity relative to the other vibronic bands when water is added to the expansion, suggesting that it belongs to a DMB/H_2O complex, a DMB molecule to which one or more water molecules are attached. Replacing the H_2O with D_2O leads to further changes in the structure of this band as shown in the insert to Figure 1. The band is fragmented, which may be attributed to isotopic exchange.

An unambiguous determination of the structure of DMB responsible for Band A was made possible by a study of the spectrum at high resolution. Figure 2 shows the rotationally resolved $S_1 \leftarrow S_0$ fluorescence excitation spectrum of Band A recorded in a molecular beam. It spans approximately 4 cm^{-1} and displays two well-defined branches. The lower frequency region of the spectrum is the P-branch ($\Delta J = -1$ transitions) and the higher frequency region is the R-branch ($\Delta J = +1$ transitions). These branches are separated by a "zero gap", where the center (or origin) of the band is located. The lack of central

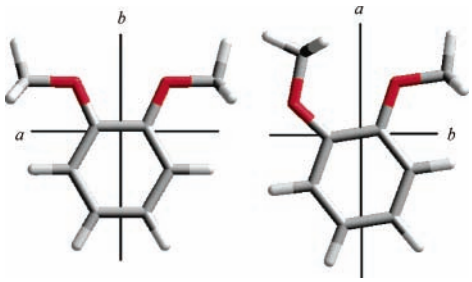

Figure 3. Two likely conformations of 1,2-dimethoxybenzene with their respective inertial axes, *trans* (left) and *cis* (right).

Q branch ($\Delta J = 0$) transitions in this gap indicates that the spectrum is a classic *b*-type spectrum.

Rotational analysis of this spectrum was performed with the jb95 program,[24] which utilizes the rigid rotor Hamiltonian:

$$H_r = AP_a^2 + BP_b^2 + CP_c^2 \quad (1)$$

Here, P_a^2, P_b^2 and P_c^2 are the components of the angular momentum about the *a*, *b*, and *c* inertial axes; *A*, *B*, and *C* are the respective rotational constants, $A = (\hbar/4\pi I_a)$, *etc.*; and I_a, I_b, and I_c are the principal moments of inertia about these axes. The fitting process began with the simulation of a spectrum using an assumed structure of DMB in both electronic states and a band type. From the appearance of the spectrum, *b*-type selection rules ($\Delta J = 0, \pm 1$, $\Delta K_a = \pm 1$, and $\Delta K_c = \pm 1$) were assumed. The structures of the ground state were taken from *ab initio* calculations, using Møller−Plesset 2nd order perturbation theory (MP2) with a 6-31G** basis set.[25] The two lowest energy structures (*trans* and *cis*) are displayed in Figure 3. They differ in energy by ~900 cm^{-1} with the *trans* isomer lying at lower energy. Clearly, the two structures have different rotational constants, providing a basis for their distinction.

Single transitions were selected from the simulation that corresponded to the experimental spectrum and were used for initial assignments. Further improvements were made by assigning $K = 0$ and 1 transitions because their intensities were expected to be strong. These assignments were iteratively optimized by a least-squares analysis routine. At a maximum *J* of 40 with the rotational temperature of 2.9 K, approximately 300 rovibronic transitions were assigned resulting in an OMC (observed minus calculated frequency) of 3.3 MHz. Finally, single transitions in the spectrum were fit to a line shape (Voigt profile) with Dopper-broadened Gaussian and lifetime-broadened Lorentzian components. The spectrum of a heavily congested portion of the R branch at full resolution is shown in Figure 4 to illustrate the quality of the fit. Individual lines have full width at half-maximum (FWHM) line widths of ~45(±5) MHz; the line shape analysis yields a Gaussian line width of 18 MHz and a Lorentzian line width of 40 MHz, corresponding to a lifetime of 4 ns.

The results of the rotational analysis are listed in Table 2 together with the calculated rotational constants. The results show unambiguously that the isomer responsible for Band A is *trans*-DMB.

TABLE 2: Ground State Rotational Constants of Band A Compared to the *ab Initio* values of *trans*- and *cis*-DMB (MP2/6-31G)**

Parameter	Band A	*trans*-DMB	*cis*-DMB
A″, MHz	1663.1(1)	1663.1	1752.0
B″, MHz	1349.8(1)	1349.6	1367.9
C″, MHz	752.6(1)	752.1	775.7
$\Delta I''$, amu Å^2	−6.80	−6.39	−6.37

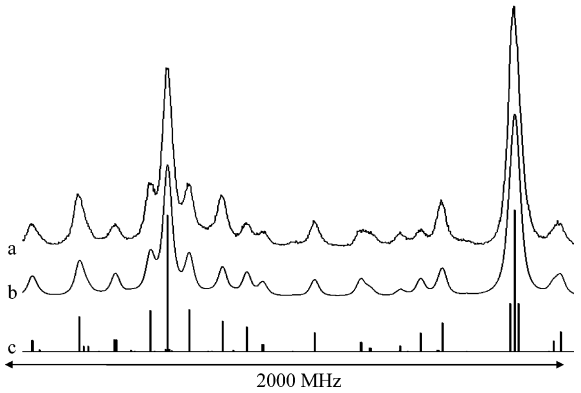

Figure 4. Portion of the R-branch taken from the spectrum of Band A of DMB at full resolution. Trace a is the experimental spectrum. Trace b is a simulated spectrum using a Voigt line shape function (18 MHz Gaussian and 40 MHz Lorentzian). Trace c is a stick figure representation of the spectrum.

Once the identity of the carrier of Band A was established, the recorded spectra of Bands B through G also were analyzed. All of these bands exhibit the same *b*-type bands as Band A. Further, the ground state rotational constants of all of these bands are the same as those for Band A, as shown in Table 3. This clearly indicates that these bands originate from the same zero point vibrational level (ZPL) in the electronic ground state, and that the isomer which is responsible for these bands is also *trans*-DMB. However, the excited state rotational parameters are all different, showing that these bands terminate in levels of the S_1 state having different vibrational characters.

Additional properties of the excited state are noted in Table 3. The differences in rotational constants ($\Delta A = A' - A''$), ΔB, and ΔC are all negative. Since rotational constants are inversely proportional to the moments of inertia ($I_a = \sum m_i(b_i + c_i)$, *etc.*), which in turn are sensitive to the displacements of atomic masses, the observed decreases in the constants are a direct result of expansion of the molecule with respect to each of the principal axes in the excited state. In addition, the magnitude of the inertial defect (ΔI) (defined as $\Delta I = I_c - I_b - I_a$) is a measure of the molecule's planarity. A rigidly planar molecule has an inertial defect of zero. As atoms deviate from the plane, the inertial defect becomes more negative. In-plane and out-of-plane vibrational motions drive the inertial defect toward more positive and negative values, respectively. The source of the inertial defect in ground state *trans*-DMB (−6.80 amu Å) is the out-of-plane hydrogens of the two methyl groups. In the excited state, the inertial defect increases in magnitude by 0.88 amu Å^2. Thus, DMB distorts along some out-of-plane coordinate and becomes less planar in the S_1 state.

The DMB/H_2O complex band, at 0_0^0 +127 cm^{-1}, also was recorded in the molecular beam. Its rotationally resolved $S_1 \leftarrow S_0$ fluorescence excitation spectrum is shown in Figure 5. The appearance of this spectrum is very different from that of the bare molecule. Now the spectrum displays a strong central Q-branch ($\Delta J = 0$ transitions), suggesting an *a*-type band. Rotational analysis of this band was performed with the jb95 program[24] that utilizes the nonrigid rotor Hamiltonian

$$H = H_r + H_d$$

$$H_d = \Delta_J P^4 - \Delta_{JK} P^2 P_a^2 - \Delta_K P_a^4 - 2\delta_J P^2 (P_b - P_c) - 2\delta_k [P_a^2 (P_b^2 - P_c^2) + (P_b^2 - P_c^2) P_a^2] \quad (2)$$

Here, H_r is the rigid rotor Hamiltonian defined in eq 1, and H_d

TABLE 3: Derived Rotational Constants from the Fits of Bands A through G in the Fluorescence Excitation Spectrum of DMB (*cf.* Figure 1)[a]

		Bands						
		A	B	C	D	E	F	G
S_0	A''	1663.1(1)	1662.9(1)	1663.0(1)	1663.1(1)	1662.9(1)	1662.9(1)	1663.2(1)
	B''	1349.8(1)	1349.7(2)	1349.9(2)	1349.9(2)	1349.7(1)	1349.7(2)	1350.0(2)
	C''	752.6(1)	752.6(1)	752.6(1)	752.6(1)	752.6(1)	752.6(1)	752.6(1)
	$\Delta I''$	−6.80	−6.80	−6.77	−6.77	−6.90	−6.80	−6.73
S_1	A'	1641.6(1)	1642.8(1)	1641.3(1)	1634.7(1)	1640.2(1)	1639.0(1)	1640.9(1)
	B'	1329.1(1)	1330.3(1)	1331.5(2)	1333.8(2)	1330.9(1)	1330.6(2)	1330.3(2)
	C'	742.7(1)	746.2(1)	745.4(1)	744.3(1)	744.4(1)	744.0(1)	742.8(1)
	$\Delta I'$	−7.68	−10.23	−9.46	−9.06	−8.95	−8.87	−7.50

[a] Rotational constants in MHz, inertial defects in amu Å^2.

is the distortion Hamiltonian, introduced by Watson[26] and discussed in more detail by Gordy and Cook.[27] Δ_J, Δ_{JK}, Δ_K, δ_j, and δ_k are the quartic distortion coefficients, and the total angular momentum (P^2) is equal to the sum of P_a^2, P_b^2, and P_c^2.

Not knowing the structure of DMB−H_2O, the bare molecule rotational constants and *a*-type selection rules ($\Delta J = 0, \pm 1$, $\Delta K_a = \pm 0$, and $\Delta K_c = \pm 1$) were used to generate an initial simulated spectrum. This was then refined, using a strategy similar to that discussed earlier, by comparison with the experimental results. Initially, a rigid rotor Hamiltonian was assumed; however, the assignments resulted in a large standard deviation (OMC ∼15 MHz). When the Watson distortion terms were then incorporated into the fit, an assignment of 560 lines yielded an OMC of 3.3 MHz. Despite the quality of this fit, the experimental spectrum still had observed transitions that were missing from the simulated spectrum. An autocorrelation analysis[28] was then performed to assess to whether multiple bands might be present. This analysis demonstrated that there are a few possible repetitive separations in the spectrum: 1.2, 2.6, and 3.7 GHz. Among these, the peak at 1.2 GHz is the most intense.

Given this result, a second simulated spectrum was generated, using the rotational constants from the main band. The initial position of origin of the second band was placed at 1.2 GHz to the blue of the first. Manipulating the origin to determine a crude frequency position, simulated rovibronic transitions were then assigned. Again distortion terms were implemented in the final assignment of 355 lines resulting in an OMC of 4.0 MHz. The fit of the spectrum was compared with Voigt profiles convoluting the two subbands; a careful measurement of the relative intensities of the two subbands gave a 3:1 ratio, within ±5%.

A portion of the R branch in the spectrum of DMB/H_2O is shown at full resolution in Figure 6. The top trace (Figure 6a) is the fluorescence excitation spectrum with individual lines having FWHM line widths of 40 ± 5 MHz. Parts c and d of Figure 6 show the contributions to this spectrum from the two subbands. Finally, Figure 6b shows the quality of the fit with the Voigt profile composed of a Gaussian line width of 18 MHz and a Lorentzian line width of 40 MHz, convoluting the two subbands. The complete inertial parameters for both electronic states are listed in Table 4. Note that these parameters are very different from those of the bare molecule (Table 3).

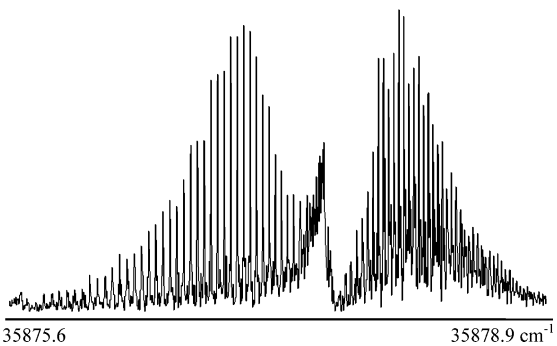

Figure 5. Rotationally resolved $S_1 \leftarrow S_0$ fluorescence excitation spectrum of 1,2-dimethoxybenzene/H_2O.

Figure 7 shows the rotationally resolved $S_1 \leftarrow S_0$ fluorescence excitation spectrum of the D_2O complex band. This spectrum displays an *a*-type band very similar to that of the H_2O complex, slightly red shifted by 0.6 cm^{-1} relative to that of DMB/H_2O. The spectrum in Figure 7 was fit by starting with the same constants as the water complex for the initial simulations, and then iterated as described before. At full resolution, a portion of the fitted R-branch is shown in Figure 8. Two simulated spectra were also required to fit the experimental spectrum. Their intensity ratio is 1:2 within ±5%. The weaker intensity band (*B* subband) is red shifted by only 45 MHz relative to stronger band (*A* subband). Voigt profiles composed of a Gaussian line width of 18 MHz and a Lorentzian line width of 40 MHz were required to fit both subbands. The final results of this fit are listed in Table 5.

IV. Discussion

We have determined the rotational constants of the ground and excited electronic states of DMB and DMB/H_2O and the orientation of the $S_1 \leftarrow S_0$ electronic transition moments in both species. We begin with a discussion of the structure of the isolated molecule, in its ground state.

The Bare Molecule, DMB. Anisole (Scheme 2), the parent molecule, has the ground state rotational constants $A = 5028.867$

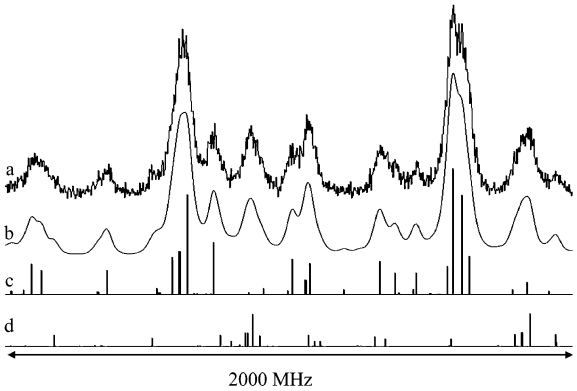

Figure 6. At full resolution, a portion of the R-branch is shown from the spectrum of 1,2-dimethoxybenzene/H_2O. Trace a is the experimental spectrum, and traces c and d show the calculated rovibronic transitions in subbands *B* and *A*, respectively. Trace b is the simulated spectrum, using the Voigt line shape function described in the text.

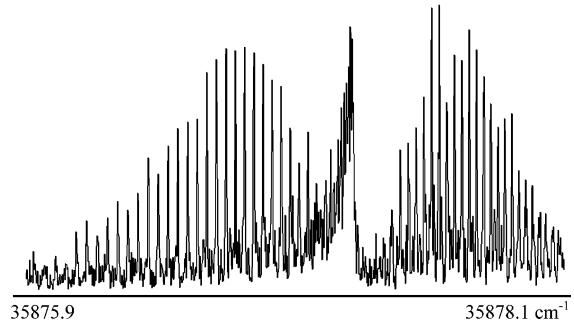

Figure 7. Rotationally resolved $S_1 \leftarrow S_0$ fluorescence excitation spectrum of 1,2-dimethoxybenzene/D_2O.

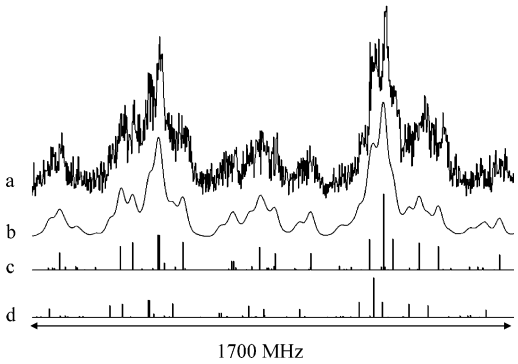

Figure 8. At full resolution, a portion of the R-branch is shown from the spectrum of 1,2-dimethoxybenzene/D_2O. The top trace is the experimental spectrum and the bottom traces c and d show the simulated rovibronic transitions in subbands *A* and *B*, respectively. Trace b is the simulated spectrum, using the Voigt line shape function described in the text.

MHz, B = 1568.375 MHz, and C = 1205.836 MHz as determined by microwave spectroscopy.[29] As shown in Table 2, the ground state rotational constants of DMB are drastically different; A = 1663.1 MHz, B = 1349.8 MHz, and C = 752.6 MHz. The substantially larger A rotational constant of anisole is due to its smaller moment of inertia; this is a direct result of the relatively small displacements of atoms perpendicular to the *a*-axis. Monosubstituted benzenes typically have much larger A than B and C constants.[30] In contrast, the displacement of the atoms from the *a* and *b* axes is more evenly distributed in DMB, and the rotational constants are more nearly equal.

TABLE 4: Rotational and Centrifugal Distortion Constants of the A and B Subbands in the $S_1 \leftarrow S_0$ Spectrum of DMB/H_2O[a]

		A subband	*B* subband
S_0 state	A''	1356.0(3)	1357.6(2)
	B''	880.7(1)	880.6(1)
	C''	538.1(1)	538.0(1)
	Δ_J''	−0.00027(9)	0.000109(3)
	Δ_{JK}''	0.0128(6)	0.00845(2)
	Δ_K''	−0.061(4)	−0.0070(1)
	δ_j''	0.00009(4)	0.000030(2)
	δ_k''	−0.0041(5)	0.00422(2)
S_1 state	A'	1335.4(3)	1337.0(2)
	B'	874.1(1)	874.0(1)
	C'	533.5(1)	533.4(1)
	Δ_J'	−0.0001(1)	0.000052(3)
	Δ_{JK}'	0.0081(6)	0.00438(2)
	Δ_K'	−0.056(4)	−0.0028(1)
	δ_j'	0.00015(5)	0.000030(2)
	δ_k'	−0.0049(5)	0.00204(2)

[a] All constants in MHz. The separation of the two subbands is 1197.10 MHz (0.04 cm^{-1}).

SCHEME 2: The Structure of Anisole with Its Inertial Frame

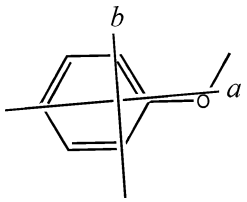

SCHEME 3: Kekulé Structures of *trans*-DMB

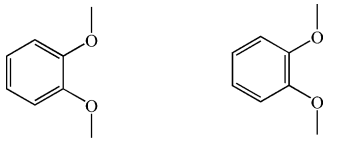

I II

Inertial defects also may be used to provide information about structure. Thus, anisole in its ground state has an inertial defect of −3.41 amu Å^2[2,29] whereas DMB in its ground state has an inertial defect of −6.80 amu Å^2. Since this value is twice as large as that for anisole, we can conclude that the atoms responsible for the nonzero values are the out-of-plane hydrogens of the methoxy substituent(s). The heavy atom structure of both molecules is planar.

An important contributor to the planar geometry of DMB is the conjugation between the methoxy lone pairs and the benzene π-orbitals. Rumi and Zerbi[31] have demonstrated that the methoxy group generates a mesomeric effect in anisole derivatives. We can easily imagine a similar effect occurring in DMB, inducing bond length alternations in the benzene ring. Thus, as shown in Scheme 3, the two canonical structures **I** and **II** do not contribute equally, with structure **I** being favored, as shown in the calculations of Krygowski *et al*.[32] In addition, canonical structure **I** has its out-of-plane hydrogens in a staggered orientation with respect to the double bond, as observed in anisole[29,32] and *cis*-methyl vinyl ether (MVE).[33] In the minimum energy geometry of structure **I**, the hydrogens are oriented toward the π cloud (Scheme 4). The calculated barrier to internal rotation of the methyl group in *cis*-MVE is 1339.5 cm^{-1} (3.83 kcal/mol).[30] A barrier on the order of 1000 cm^{-1} will produce a tunneling splitting on the order of 10 MHz in an electronic spectrum, making it difficult to observe.

TABLE 5: Rotational and Centrifugal Distortion Constants of the A and B Subbands in the $S_1 \leftarrow S_0$ Spectrum of DMB/D_2O[a]

		A subband	*B* subband
S_0 state	A''	1356.1(4)	1356.0(6)
	B''	846.6(1)	846.6(1)
	C''	525.2(1)	525.4(1)
	Δ_J''	0.0008(1)	0.0003(2)
	Δ_{JK}''	0.0027(7)	0.008(1)
	Δ_K''	0.008(6)	0.002(8)
	δ_j''	0.00022(6)	0.00024(8)
	δ_k''	0.0054(9)	0.007(2)
S_1 state	A'	1335.0(4)	1334.9(6)
	B'	840.3(1)	840.4(1)
	C'	521.4(1)	521.2(1)
	Δ_J'	0.0008(1)	0.0005(2)
	Δ_{JK}'	−0.0015(8)	0.004(1)
	Δ_K'	0.012(6)	0.006(8)
	δ_j'	0.00026(6)	0.00035(8)
	δ_k'	0.0037(9)	0.006(2)

[a] All constants in MHz. The separation of the two subbands is 45.4 MHz (0.0015 cm^{-1}).

SCHEME 4: Orientation of the Methyl Hydrogens in *cis*-MVE

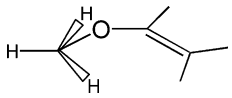

Excitation of DMB to its S_1 state produces large changes in its rotational constants: $\Delta A = (A' - A'') = -21.5$ MHz (1.3%), $\Delta B = -20.7$ MHz (1.5%), and $\Delta C = -9.9$ MHz (1.3%). All values are negative, suggesting an expansion of the molecular frame. An increase in molecular size is a natural consequence of excitation by light, since antibonding orbitals are populated and bonding orbitals are depopulated. However, the ΔA, ΔB, and ΔC values in DMB are all of the same magnitude, whereas typical monosubstituted benzenes exhibit much larger ΔA values compared to ΔB and ΔC. For example, aniline has $\Delta A = -331.2$ MHz, $\Delta B = 39.6$ MHz, and $\Delta C = -17.8$ MHz, revealing significant bond lengthening in directions perpendicular to the *a*-axis.[34] The quinoidal model first proposed by Cvitas[35] and shown in Scheme 5 seems to account for these changes.

SCHEME 5: Structural Changes in Monosubstituted Benzenes on S_1 Excitation

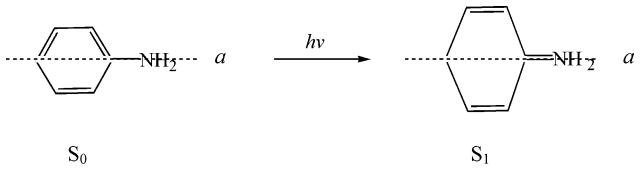

S_0 S_1

Clearly, DMB is different; the primary C_2 symmetry axis is now along the *b* inertial axis rather than *a*. This explains the differences in its ΔA, ΔB, and ΔC values. We have explored the possible structural changes using *ab initio* methods, MP2 with a 6-31G** basis set for the S_0 state and CIS with a 6-31+G* basis set for the S_1 state. The calculations reproduce well the *A*, *B*, and *C* values of the S_0 state, and the ΔA, ΔB, and ΔC values of the S_1 state. Hence, they should be reliable indicators of the geometries of the two states. Figure 9 shows the results obtained. The major changes on electronic excitation are in the C_1-O_1 and C_6-O_2 bond lengths; these decrease from 1.368 to 1.328 Å. The $C_1-O_1-C_7$ and $C_6-O_2-C_8$ bond angles increase from 116.1° to 121.1°. In the ring, the C_1-C_2 and C_5-C_6 bond lengths increase from 1.394 to 1.431 Å. The observed changes in structure are consistent with those shown schematically in Scheme 6, below.

The calculations also provide some insight into the changes in electronic distribution that occur on excitation of the S_1 state. Shown in Scheme 7 are two of the relevant orbitals, HOMO (highest occupied molecular orbital) and LUMO (lowest unoccupied molecular orbital) that participate in the $S_1 \leftarrow S_0$ electronic transition. Clearly, absorption of a photon introduces antibonding character into the C_1-C_2 and C_5-C_6 bonds and increases the electron density at C_2 and C_5. Also, the electron density decreases at all remaining heavy atoms, especially the O_1 and O_2 atoms. These changes, in turn, produce changes in the equilibrium geometries of the two states; those shown in Scheme 6 are consistent with those shown in Scheme 7. We also see from Scheme 7 that the light induced oscillations of electron density occur mainly along *b*, explaining why the 0_0^0 band of *trans*-DMB is *b*-axis polarized. The observed TM orientation in DMB is consistent with the observed S_1-S_0 TM orientations of a large variety of other substituted benzenes.[36]

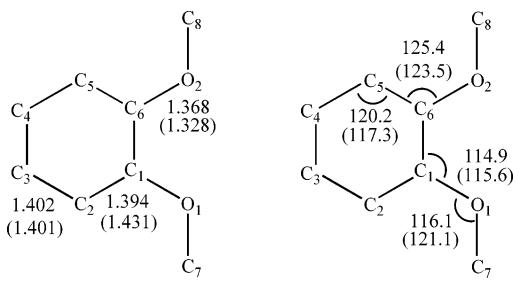

Figure 9. *Ab initio* geometries of DMB in its S_0 and S_1 states. S_1 state values are given in parentheses with bond lengths in Å (left) and angles in deg (right).

SCHEME 6: Structural Changes in *trans*-DMB on S_1 Excitation

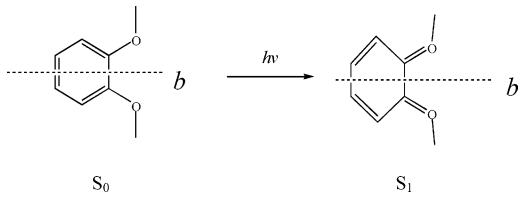

S_0 S_1

SCHEME 7: CIS/6-31G* Calculated One-Electron Molecular Orbitals of DMB

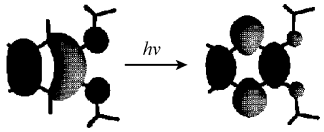

S_0 (HOMO) S_1 (LUMO)

The structural changes shown in Scheme 6 also explain the substantial vibrational activity that appears in the low resolution S_1-S_0 spectrum of DMB (Figure 1). To further evaluate the nature of these vibrations, normal mode calculations were performed on S_0 DMB using the 6-31G* basis set. *trans*-DMB has 54 normal modes; the five lowest fundamental vibrational frequencies are at 71, 87, 150, 173, and 212 cm^{-1} (these values were scaled by the multiplicative factor of 0.89). A careful examination of the atomic displacements in each mode shows two dimethoxy in-phase, out-of-plane bending modes at 71 ($b_1^{\dagger}$) and 212 ($b_1^{\ddagger}$) cm^{-1}, two out-of-phase modes at 87 ($a_2^{\dagger}$) and 150 ($a_2^{\ddagger}$) cm^{-1}, and an in-plane symmetric bending mode (a_1) at 173 cm^{-1}, as shown in Scheme 8. Thus, we tentatively assign Band B (at +84.2 cm^{-1}) as the first overtone of an out-of-plane bending mode ($b_1^{\dagger}$ or $a_2^{\dagger}$) since it exhibits the largest (in magnitude) inertial defect (−10.23 amu Å^2). Band G (at +201.8 cm^{-1}) can be assigned to the in-plane bending mode (a_1 symmetry) since it exhibits the smallest inertial defect (−7.50 amu Å^2). Other bands have been assigned as overtones and combinations of these modes as shown in Table 1.

The Water Complex, DMB−H_2O. The $S_1 \leftarrow S_0$ electronic transition moment of DMB is oriented along the *b*-axis in the plane of the molecule as shown in Scheme 9. The corresponding transition in DMB/water has its transition moment parallel to *a*. Given the relatively weak nature of the intermolecular bond(s) between the two species, attachment of the water molecule is not likely to change the nature of the S_1-S_0 electronic transition. Therefore, the most likely H_2O bonding site is along *b*, nestled between the two methoxy groups (see Scheme 9). Owing to its increased mass, the attachment of the weakly bound water exchanges the two inertial axes, *a* and *b*, resulting in an *a*-type origin band in DMB−H_2O.

SCHEME 8: Low-Frequency Vibrations of DMB in the Ground State

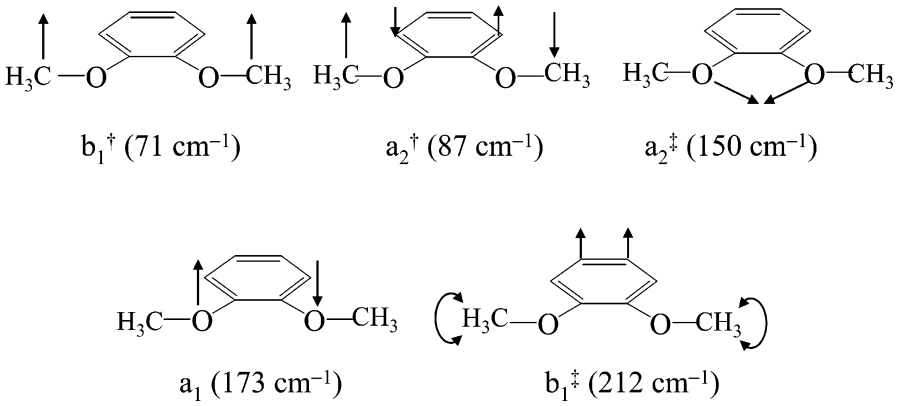

SCHEME 9: The TM Orientation of DMB and Its Water Complex Are Indicated by an Arrow

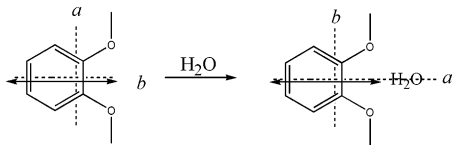

Further evidence for this binding site comes from the observed rotational constants. If the water moiety lies on the *b*-principal axis of the bare molecule, then that particular rotational constant will remain unchanged upon complexation. The rotational constants of DMB and the water complex are compared in Table 6. Those of the bare molecule are larger than those of the complex, of course; the reduction is due to the addition of the water molecule. But the average *A* rotational constant of the two subbands of the complex is close to the *B* rotational constant of the bare molecule. This shows that the water molecule lies on the *b*-axis of the bare molecule. Also notice that the differences in the excited state rotational constants, ΔB of the bare molecule and ΔA of the complex, are identical, confirming this conclusion. Further, the relatively small inertial defects of the complex suggest that the water lies in the plane of DMB. The small differences in the inertial defects can be accounted for by out-of-plane hydrogen atoms of the water molecule.

More quantitatively, we have determined the COM coordinates of the attached water molecule using the Kraitchman method.[27] The results are listed in Table 7 and shown approximately in Scheme 10. According to this analysis, the water molecule lies well outside the two methoxy groups at a distance of 4.05 Å along the *a* axis in the ground state. This distance decreases slightly on excitation of DMB to its S_1 state, but this

TABLE 6: Rotational Parameters of DMB and the DMB−H_2O Complex. The Values for the Complex Are the Average Values of Two Subbands[a]

DMB			DMB/H_2O
A''	1663.1	A''_H	1356.8
B''	1349.8	B''_H	880.7
C''	752.6	C''_H	538.1
$\Delta I''$	−6.80	$\Delta I''_H$	−7.1
A'	1641.6	A'_H	1336.2
B'	1329.1	B'_H	874.1
C'	742.7	C'_H	533.5
$\Delta I'$	−7.68	$\Delta I'_H$	−9.12
ΔA	−21.5	ΔA_H	−20.6
ΔB	−20.8	ΔB_H	−6.6
ΔC	−9.9	ΔC_H	−4.6

[a] Rotational constants in MHz, inertial defects in amu Å^2.

SCHEME 10: Circles Indicate the Four Equivalent Positions of the COM of the Attached Water Molecule in the *ab* and *bc* Planes of DMB/H_2O

decrease in *a* is likely caused by expansion of the bare molecule, not a tighter binding of the attached H_2O. (The DMB/H_2O origin band is blue shifted by 127 cm^{-1} with respect to that of the bare molecule, indicating a weaker intermolecular interaction in the S_1 state.) The coordinate $|b|$ is substantially different from zero in both states. Apparently, the water molecule is localized on one side of the *ac* plane or the other. In contrast, the coordinate $|c|$ is significantly smaller, suggesting a large amplitude motion perpendicular to the *ab* plane.

Information about the orientation of the attached water molecule and the position of its hydrogen atoms comes from a similar comparison of the rotational constants of DMB/H_2O and DMB/D_2O. This comparison is shown in Table 8. Examining these results, we see that deuterium substitution produces a large change in *B* and *C*, but only a small change in *A*. The large change in *B* is a direct consequence of the larger displacement of the water molecule from the *b* axis (*cf.*, Table 7) and is a "trivial" result. But the fact that deuterium substitution produces

TABLE 7: Kraitchman Coordinates (in Å) of the Center-of-Mass (COM) of Water in Both Electronic States of DMB/H_2O[a]

Coordinate	S_0	S_1
$\|a\|$	4.053(5)	4.029(5)
$\|b\|$	0.61(2)	0.68(2)
$\|c\|$	0.14(7)	0.29(3)
$\|r\|$	4.100(1)	4.098(1)

[a] *a*, *b*, and *c* are the inertial axes of the complex.

TABLE 8: Rotational Constants (in MHz) of DMB/H_2O, DMB/D_2O, and Their Differences[a]

		H_2O		D_2O		H_2O-D_2O
S_0	A''_H	1356.8	A''_D	1356.0	A''_{H-D}	−0.8
	B''_H	880.7	B''_D	846.6	B''_{H-D}	−34.1
	C''_H	538.1	C''_D	525.5	C''_{H-D}	−12.6
S_1	A'_H	1336.2	A'_D	1335.0	A'_{H-D}	−1.2
	B'_H	874.1	B'_D	840.4	B'_{H-D}	−33.7
	C'_H	533.5	C'_D	521.3	C'_{H-D}	−12.2

[a] The values shown are the average values for the two subbands in each electronic state.

TABLE 9: Disubstituted Kraitchman Analysis[a]

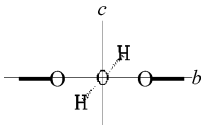

	S_0	S_1
$\|a\|$	3.378	3.365
$\|b\|$	0.335	0.426
$\|c\|$	0.453	0.591
H···H	1.127	1.456

[a] The coordinates (in Å) are the locations of hydrogen atoms determined from a comparison of the rotational constants of DMB/H_2O and DMB/D_2O. The H···H distance is calculated from these coordinates. (The actual H···H distance in water is 1.536 Å)[27]

a much larger change in *C* than in *A* is a nontrivial result. This result demonstrates that the water hydrogens are tilted out of the *ab* plane and make a much larger projection on *c* than *a*. Each methoxy group oxygen has two lone pairs of electrons, pointing above and below the *ab* plane. Thus, the hydrogens of the attached water molecule are most probably hydrogen bonded to two of these lone pairs, one above the *ab* plane and the other below.

Table 9 lists the hydrogen atom coordinates that were derived from a comparison of the rotational constants of the two complexes. In accord with our expectation, the plane of the water molecule is tilted with respect to the *b* and *c* axes, so that one hydrogen lies above the *ab* plane and one lies below. The hydrogen atoms are "inside" the water oxygen (*cf*., Table 7), making donor hydrogen bonds with one of the two methoxy oxygen lone pairs, one above and one below. The H−H distance in the water molecule that is projected onto the *bc* plane of the complex is 1.13 Å in the S_0 state (1.46 Å in the S_1 state), compared to an actual separation of 1.536 Å.[27]

Water Motion in DMB/H_2O. The two subbands in the fluorescence excitation spectrum of DMB/H_2O arise from a hindered internal motion of water. The motion of water perturbs and splits the degenerate torsional level ($v = 0$) into nondegenerate subtorsional levels ($\sigma = 0$ and 1) in the 2-fold potential energy surface, resulting in different energy level separations in the ground and excited electronic states. This is shown schematically in Figure 10. Allowed transitions $A \leftrightarrow A$ and $B \leftrightarrow B$ (according to the selection rule) are responsible for the *A* and *B* subbands, respectively. In DMB/H_2O, the two subbands are split by 1197 MHz (0.04 cm^{-1}). The *A* subband is blue shifted relative to the *B* subband. This indicates that the subtorsional level splitting in the S_1 state is smaller than that in the S_0 state. Thus, the excited state barrier (V_2') is larger than the ground state barrier (V_2''). The two subbands have different relative intensities, 3:1. This intensity difference has its origin in nuclear spin statistical weights. Thus, the motion of the attached H_2O interconverts the two protons, making them equivalent.

The intensity difference of the two subbands (3:1) comes from nuclear spin statistical weights. Ordinary water has a pair of identical hydrogen nuclei ($I = {}^1/_2$). The total wave function of the molecule (Ψ_T) is comprised of electronic (Ψ_E), vibrational (Ψ_V), rotational (Ψ_R), and nuclear spin (Ψ_{ns}) wave functions. Ψ_T must be antisymmetric with respect to exchange of the two nuclei since they are fermions. Ψ_E is symmetric and Ψ_V is either symmetric (*A* subtorsional level) or antisymmetric (*B* subtorsional level). The rotational wave function (Ψ_R) is either symmetric (*ee* or *oo*) or antisymmetric (*eo* or *oe*). Since there are three symmetric spin functions and one antisymmetric,

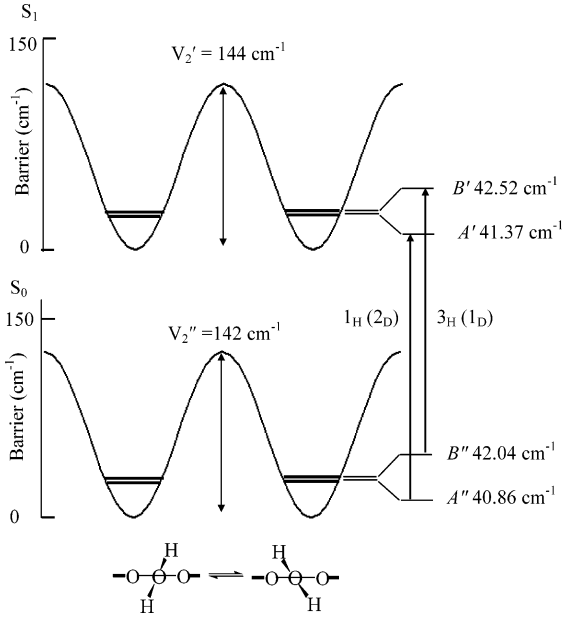

Figure 10. Potential energy surfaces of DMB/water in its two electronic states plotted as a function of the water torsional coordinate. The two minima arise from two equivalent orientations of the attached H_2O. Tunneling along this coordinate gives rise to symmetry distinguishable torsional substates A and B. Allowed transitions between these two states are indicated by arrows with their corresponding intensity ratios.

rotational levels belonging to the *A* subtorsional level have a statistical weight of one and rotational levels belonging to the *B* subtorsional level have a statistical weight of three. In DMB/D_2O, the nuclear spin wave function for subtorsional Band A is symmetric and that for subtorsional Band B is antisymmetric, leading to a 2:1 intensity ratio.

Motion of the water molecule also changes the effective rotational constants of the complex.[37] The difference between the rotational constants of the subtorsional levels are $\Delta A''_{v\sigma} = A''_{01} - A''_{00}$. The values in DMB−water are $\Delta A''_{v\sigma} = 1.7 \pm 0.9$ and $\Delta A'_{v\sigma} = 1.6 \pm 0.9$ MHz. The $\Delta B_{v\sigma}$ and $\Delta C_{v\sigma}$ values are significantly smaller, less than 0.2 MHz, suggesting that the axis about which the water moves is nearly parallel to the *a*-axis of the complex. A quantitative approach to this problem is represented by the effective rotational Hamiltonian,[27]

$$H^{\text{eff}}_{v\sigma} = A_{v\sigma}P_a^2 + B_{v\sigma}P_b^2 + C_{v\sigma}P_c^2 \qquad (3)$$

where $A_{v\sigma}$ *etc*. are effective rotational constants given by

$$A_{v\sigma} = A + FW^{(2)}_{v\sigma}\rho_a^2, \textit{ etc.} \qquad (4)$$

Here, *A* is the rigid rotor rotational constant, *F* is the reduced rotational constant for internal rotation ($=\hbar^2/2rI_\alpha$), $W^{(2)}_{v\sigma}$ is a second-order perturbation constant,[38] and ρ_a is a weighted direction cosine of the angle between the axis of the internal rotor and the *a* principal axis of the complex, $\rho_a = \lambda_a(I_\alpha/I_a)$. I_α is the moment of inertia of the attached top, and *r* is a reduction factor

$$r = 1 - \sum \frac{\lambda_g^2 I_\alpha}{I_g}, \qquad g = a, b, c \qquad (5)$$

Projecting the symmetry axis of the water molecule onto the *a*-axis of the complex, the reduced rotational constant (*F*) is calculated to be 436.7 GHz in both states. Then, to determine

TABLE 10: Internal Rotation Parameters of DMB/H_2O

	S_0	S_1
ΔA (MHz)	1.7 ± 0.9	1.6 ± 0.9
λ_a/α (deg)	1/0	1/0
F (GHz)	436.71	436.71
$W_{\nu\sigma}^{(2)}$	0.408	0.389
s	9.75	9.88
V_2 (cm^{-1})	142 ± 50	144 ± 50
subtorsional split (cm^{-1})	1.18 ± 0.63	1.15 ± 65

the barrier height, the difference ΔA was set equal to $FW_{\nu\sigma}^{(2)}\rho_a^2$, and the second-order correction terms $W_{\nu\sigma}^{(2)}$ were calculated, from which (using Herschbach's tables[38]) the reduced barriers and 2-fold barrier heights V_2 were determined. The results of these calculations are shown in Table 10. We find $V_2'' = 142 \pm 50$ cm^{-1} and $V_2' = 144 \pm 55$ cm^{-1}, nearly the same values in both electronic states. The calculated subtorsional band splittings yield a tunneling of splitting 0.03 ± 0.90 cm^{-1} that agrees with the experimental value of 0.04 cm^{-1}. The MP2/6-31G** value of the torsional barrier is $\sim$450 cm^{-1}.

V. Conclusions

Rotationally resolved fluorescence excitation spectra of 1,2-dimethoxybenzene (DMB) and its single water complex DMB/H_2O have been observed and assigned. This analysis shows that the methoxy groups of DMB lie in the plane of the aromatic ring in a *trans*-disposed fashion, with the methyl groups being staggered relative to the benzene ring. This configuration provides a unique binding site for a single water molecule in DMB/H_2O. The water molecule is linked *via* two donor hydrogen bonds to the oxygen lone pairs of the methoxy groups. Torsional subbands appear in the spectrum of DMB/H_2O showing that the attached water molecule moves within the complex from one set of lone pairs to the other. The potential barriers to this motion have been measured: $V_2'' = 142 \pm 50$ cm^{-1} and $V_2' = 144 \pm 55$ cm^{-1} in the two electronic states.

Acknowledgment. This work has been supported by NSF (CHE-0315584) to whom we are grateful.

References and Notes

(1) Dibello, L. M.; McDevitt, H. M.; Roberti, D. M. *J. Phys. Chem.* **1968**, *72*, 1405.
(2) Hill, W. G.; Mason, S. F.; Peacock, R. D. *J. Chem. Soc., Perkin II* **1977**, 1262.
(3) Anderson, G. M.; Kollman, P. A.; Domelsmith, L. N.; Houk, K. N. *J. Am. Chem. Soc.* **1979**, *101*, 2344.
(4) Konschin, H.; Tylli, H.; Westermark, B. *J. Mol. Struct.* **1983**, *102*, 279.
(5) Yamamoto, S.; Okuyama, K.; Mikami, N.; Ito, M. *Chem. Phys. Lett.* **1986**, *125*, 1. Breen, P. J.; Bernstein, E. R.; Secor, H. V.; Seeman, J. I. *J. Am. Chem. Soc.* **1989**, *111*, 1958.
(6) Basche, T.; Brauchle, C.; Voitlander, J. *Chem. Phys. Lett.* **1988**, *144*, 226.
(7) Gerzain, M.; Buchanan, G. W.; Driega, A. B.; Facey, G. A.; Enright, G.; Kirby, R. A. *J. Chem. Soc., Perkin II* **1996**, 2687.
(8) Gutowsky, H. S.; Emilsson, T.; Arunan, E. *J. Chem. Phys.* **1993**, *99*, 4883.
(9) Pribble, R. N.; Garrett, A. W.; Haber, K.; Zwier, T. S. *J. Chem. Phys.* **1995**, *103*, 531.
(10) Fredericks, S. Y.; Jordan, K. D.; Zwier, T. S. *J. Phys. Chem.* **1996**, *100*, 7810.
(11) Melandri, S.; Consalvo, D.; Caminati, W.; Favero, P. G. *J. Chem. Phys.* **1999**, *111*, 3874.
(12) Schäfer, M.; Borst, D. R.; Pratt, D. W.; Brendel, K. *Mol. Phys.* **2002**, *100*, 3553.
(13) Becucci, M.; Pietraperzia, G.; Pasquini, M.; Piani, G.; Zoppi, A.; Chelli, R.; Castellucci, E. *J. Chem. Phys.* **2004**, *120*, 5601. Giuliano, B.; Caminati, W. *Angew. Chem., Int. Ed.* **2005,** *44*, 603. Ribblett, J.; Sinclair, W.; Borst, D.; Yi, J.; Pratt, D. *J. Phys. Chem. A.* In press.
(14) Tarakeshwar, P.; Kim, K. S.; Brutschy, B. *J. Chem. Phys.* **1999**, *110*, 8501.
(15) Barth, H. D.; Buchhold, K.; Djafari, S.; Reimann, B.; Lommatzsch, U.; Brutschy, B. *Chem. Phys.* **1998**, *239*, 49.
(16) Kang, C.-H.; Pratt, D. W.; Schäfer, M. *J. Phys. Chem. A* **2005**, *109*, 767.
(17) Berden, G.; Meerts, W. L.; Schmitt, M.; Kleinermanns, K. *J. Chem. Phys.* **1996**, *104*, 972.
(18) Korter, T. M.; Pratt, D. W.; Küpper, J. *J. Phys. Chem. A* **1998**, *102*, 7211.
(19) Braly, L. B.; Cruzan, J. D.; Liu, K.; Fellers, R. S.; Saykally, R. J. *J. Chem. Phys.* **2000**, *112* 10293. Spoerel, U.; Stahl, W. *J. Mol. Spectrosc.* **1998**, *190*, 278.
(20) Brookes, M. D.; McKellar, A. R. W. *J. Chem. Phys.* **1998**, *109*, 5823.
(21) Majewski, W. A.; Pfanstiel, J. F.; Plusquellic, D. F.; Pratt, D. W. In *Laser Techniques in Chemistry*; Myers, A. B., Rizzo, T. R., Eds.; Wiley & Sons: New York, 1995; p 101.
(22) Marjit, D.; Bishui, P. K.; Banerjee, S. B. *Indian J. Phys.* **1971**, *46*, 49.
(23) Harris, D.; Bertolucci, M. D. *Symmetry and Spectroscopy*: *An Introduction to Vibrational and Electronic Spectroscopy;* Dover Publications: New York, 1978.
(24) Described in: Plusquellic, D. F.; Suenram, R. D.; Mate, B.; Jensen, J. O.; Samuels, A. C. *J. Chem. Phys.* **2001**, *115*, 3057.
(25) Frisch, M. J.; Trucks, G. W.; Schlegel, H. B.; et al. *Gaussian 98*, Revision A.9; Gaussian, Inc.: Pittsburgh, PA, 1998.
(26) Watson, J. K. G. In *Vibrational Spectra and Structure*; Durig, J. R., Ed.; Elsevier: Amsterdam, The Netherlands, 1977; Vol. 6, p 1.
(27) Gordy, W.; Cook, R. L. *Microwave Molecular Spectra*; Wiley & Sons: New York, 1970.
(28) Helm, R. M.; Vogel, H. P.; Neusser, H. J. *Chem. Phys. Lett.* **1997**, *270*, 285.
(29) Onda, M.; Toda, A.; Mori, S.; Yamaguchi, I. *J. Mol. Struct.* **1986**, *144*, 47.
(30) Upadhyay, D. M.; Shukla, M. K.; Mishra, P. C. *J. Mol. Struct.* **2000**, *531*, 249.
(31) Rumi, M.; Zerbi, G. *J. Mol. Struct.* **1999**, *509*, 11.
(32) Krygowski, T. M.; Pietka, E.; Anulewicz, R.; Cyransk, M. K.; Nowacki, J. *Tetrahedron* **1998**, *54*, 12289.
(33) Cahill, P.; Gold, L. P.; Owen, N. L. *J. Chem. Phys.* **1967**, *48*, 1620.
(34) Sinclair, W. E.; Pratt, D. W. *J. Chem. Phys.* **1996**, *105*, 7942.
(35) Cvitas, T.; Hollas, J. M.; Kirby, G. H. *Mol. Phys.* **1970**, *19*, 305.
(36) See, for example: Selby, T. M.; Clarkson, J. R.; Mitchell, D.; Fitzpatrick, J. A. J.; Lee, H. D.; Pratt, D. W.; Zwier, T. S. *J. Phys. Chem. A* **2005**, *109*, 4484.
(37) Tan, X.-Q.; Majewski, W. A.; Plusquellic, D. F.; Pratt, D. W. *J. Chem. Phys.* **1991**, *94*, 7721.
(38) Herschbach, D. R. *J. Chem. Phys.* **1959**, *31*, 91.